Proc. of the European Safety and Reliability Conference (ESREL 2026)
Edited by José C. Matos, Paulo B. Lourenço, Michael Beer, Daniel Oliveira,
Edoardo Patelli, Hélder S. Sousa, Rui A. Silva and Monica Santamaria
 Published by Research Publishing, Singapore.
doi: 10.3850/ESREL2026061419_esrel26-p27909-cd

Computational risk assessment framework for a High Temperature Electrolysis Facility powered by Nuclear Power and exposed to seismic hazard

Stefano Marchetti

Energy Department, Politecnico di Milano, Milano 20156, Italy. E-mail: stefano.marchetti@polimi.it
Systems Risk and Reliability (SyRRA) Lab, Center for Risk and Reliability, Reliability Engineering, University of Maryland, College Park, 20742, MD, USA. E-mail: smarchet@umd.edu

Francesco Di Maio

Energy Department, Politecnico di Milano, Milano 20156, Italy. E-mail: francesco.dimaio@polimi.it

Samantha E. Wismer

Systems Risk and Reliability (SyRRA) Lab, Center for Risk and Reliability, Reliability Engineering, University of Maryland, College Park, 20742, MD, USA. E-mail: swismer@umd.edu

Katrina M. Groth

Systems Risk and Reliability (SyRRA) Lab, Center for Risk and Reliability, Reliability Engineering, University of Maryland, College Park, 20742, MD, USA. E-mail: kgroth@umd.edu

Enrico Zio

MINES Paris-PSL, Centre de Recherche sur les Risques et les Crises (CRC), Sophia Antipolis, France. E-mail: enrico.zio@minesparis.psl.eu
Energy Department, Politecnico di Milano, Milano 20156, Italy. E-mail: enrico.zio@polimi.it

High Temperature Electrolysis Facilities (HTEFs) powered by Nuclear Power Plants (NPPs) can provide a cost-efficient way for large-scale production of clean hydrogen. As safety needs to be evaluated, in this paper we present a computational risk assessment framework for the resulting integrated system. Monte Carlo Simulation with Importance Sampling (MCS-IS) is used for the generation of scenarios that may occur from the coupling of HTEFs and NPPs. An application is shown with reference to a preliminary design of an integrated hydrogen production system in which the steam and electric power produced by a NPP are supplied to the HTEF. The HTEF and NPP system of systems is assumed to be located in a region where potential seismic activity cannot be excluded. Results show that overcurrent events leading to a Loss of Heat Sink (LHS) are the main contributors to risk.
Keywords: High Temperature Electrolysis Facility (HTEF), Nuclear Power Plant (NPP), Computational risk assessment, Monte Carlo Simulation (MCS), Importance Sampling (IS).

1. Introduction

Hydrogen is a promising energy carrier in the transition toward low-carbon energy systems for industrial, transportation and storage applications (International Energy Agency 2022; U.S. Department of Energy 2023). To enable hydrogen deployment at scale while meeting decarbonization targets, international energy strategies increasingly prioritize production with low greenhouse gas emissions (Moura and Soares 2023; International Energy Agency 2022). In this regard, the coupling of High Temperature Electrolysis Facilities (HTEFs) and Nuclear Power Plants (NPPs) has emerged as a promising solution, allowing the use of

nuclear-generated electricity and high-temperature steam to achieve high hydrogen production efficiency (Chalkiadakis et al. 2023; Frick et al. 2022).

However, the coupling of HTEFs and NPPs introduces new hazards, which may increase the risk at site level (Vedros et al. 2023). Risk assessment of HTEF-coupled NPP systems is challenged by the complex interdependencies between the two systems, that can give rise to low-probability, high-consequence accidental scenarios that are difficult to figure out without a structured framework of analysis (Al-Douri and Groth 2024; Groth et al. 2024). To address this challenge, this paper proposes a computational risk assessment framework that relies on Monte Carlo Simulation combined with Importance Sampling (MCS-IS) to efficiently explore the accidental scenario space and parse out scenarios that might have been otherwise overlooked (Rubinstein 1997; Pedroni and Zio 2017; Turati et al. 2016; Futalef et al. 2025; Enrico Zio 2013). The framework is applied to a conceptual hydrogen production layout in which a NPP supplies both thermal energy and electricity to a HTEF (Westover and Boardman 2023). The case study considers a 500 MW HTEF composed of multiple Solid Oxide Electrolyzers (SOEs) coupled to a 1000 MW nuclear installation consisting of four identical Small Modular Dual Fluid Reactor (SMDFR) units. SMDFR is an innovative fast reactor design whose high operating temperatures make it ideal for hydrogen production (Huke et al. 2015). The risk assessment is focused on seismic hazard, which is a major source of risk. Results show that accidents triggered by earthquakes and occurring in the hydrogen production facility contribute to the risk profile of the co-located NPP. Such results also highlight the importance of identifying appropriate design parameters (such as the separation distance between HTEF and NPP) to mitigate the risk increase due to seismic hazard and support the licensing of the integrated plant. The novelty of the work consists in i) modelling the coupling between hydrogen production systems and nuclear facilities within a unified probabilistic risk assessment framework; ii) incorporating seismic hazard and explosion propagation mechanisms and iii) using importance sampling to efficiently estimate rare accident scenarios affecting nuclear safety.

The remainder of the paper is organized as follows: Section 2 presents the case study, Section 3 describes the computational framework, Section 4 discusses results and Section 5 draws conclusions.

2. Case study

The layout of the HTEF-coupled NPP is sketched in **Fig. 1**.

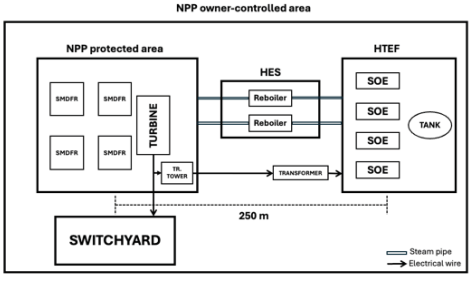

Fig. 1. Layout of HTEF-coupled NPP.

The system (of systems) comprises a NPP with $N = 4$ SMDFR, each with a nominal power of 250 MW, and a large-scale hydrogen production facility (i.e., the HTEF) with nominal rating (i.e., power input at full hydrogen production) of 500 MW.

The NPP turbine is connected to both the power grid, through a high-voltage switchyard adjacent to the NPP protected area, and to the HTEF, through a transmission tower located inside the NPP protected area. The operating parameters of the NPP are reported in **Table 1**.

Table 1. NPP operating parameters (Liu et al. 2021).

Parameter	Value
Mean linear power density	609 W/cm
Fuel inlet temperature	1300 K
Coolant inlet temperature	973 K
Steam flow rate	75 kg/s
Steam temperature	700 $°C$
Steam pressure	0.4 MPa

The HTEF is composed of several SOEs and is expected to produce up to 290 $\frac{metric\ tons}{day}$ of hydrogen. The HTEF is located outside of the NPP protected area, but inside of the owner-controlled area. For safety reasons, a separation distance of 250 m is considered between the HTEF and the NPP, and between the HTEF and the NPP high-voltage switchyard. The HTEF is equipped with a storage tank with capacity of 25 m^3 (Westover and Boardman 2023). The operating parameters of the HTEF are reported in **Table 2**.

Table 2. HTEF operating parameters (Westover and Boardman 2023; Yanxing et al. 2019).

Parameter	Value
Hydrogen production at full capacity	290 $tons/day$
Steam input flow rate at full capacity	65 kg/s
Steam input temperature	700 $°C$
Steam input pressure	0.4 MPa
Hydrogen storage temperature	110 K
Hydrogen storage pressure	70 MPa
Hydrogen storage tank volume	25 m^3

The coupling of the two systems is achieved through:

- a Heat Extraction System (HES), composed by two piping lines that route the high-temperature steam from the NPP to two steam reboilers that create steam from a deionized or demineralized water source. The steam is, then, provided to the HTEF to be used in the HTE process. The HES is equipped with several isolation valves to isolate any steam leakage;
- a transmission tower with electrical wiring to divert electrical energy, in the form of alternating current, from the output of the turbine to the HTEF, where most of the required power is converted to rectified direct current with a transformer.

In this work, we assume that the NPP is always operating at full power, whereas the variability in the energy demand is accounted for using the normalized demand of nuclear energy in the US in 2023, whose Cumulative Distribution Function (CDF) is shown in **Fig. 2** (Energy Information Administration 2023). The HTEF operates on the unused portion of the produced steam and electricity, creating a dynamic dependency between grid demand and hydrogen production capacity.

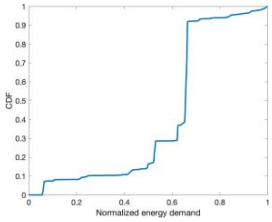

Fig. 2. Normalized energy demand CDF.

3. Computational risk assessment framework

With reference to the case study in Section 2, the computational risk assessment to estimate the site-level risk increase caused by the HTEF coupling proceeds by:

1. hazard characterization (Section 3.1);
2. system response characterization (Section 3.2);
3. core damage frequency increase estimation (Section 3.3).

3.1. Hazard characterization

We assume that the system is located in a seismic area, and we consider earthquakes with Peak Ground Acceleration (PGA) $PGA \in [0,19.62]\frac{m}{s^2}$. The magnitude-frequency curve is taken from (Shahraki and Shabakhty 2015) and shown in **Fig. 3**. It is important to note that the magnitude-frequency curve does not refer to any site-specific seismic design basis safety assessment, but it is used, without loss of generality, for the seismic hazard characterization of a hypothetical site.

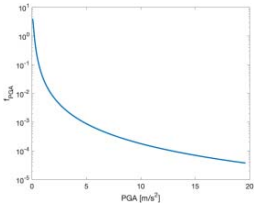

Fig. 3. Earthquake magnitude-frequency curve.

3.2. System response characterization

The effect of the earthquake on the HTEF-coupled NPP is evaluated using tailored fragility curves that provide the failure probability, P_f, for the components and safety systems exposed and vulnerable to the external stress of earthquake shocks. Specifically, for the HTEF, an earthquake can lead to the following accident Initiating Events (IEs):

- Hydrogen leakage, which can be caused by the failure of the hydrogen pipes, whose fragility curve is taken from (Smith et al. 2006) and shown in **Fig. 4**.

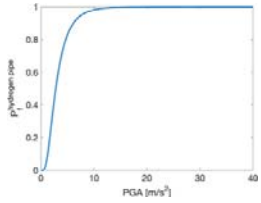

Fig. 4. Hydrogen pipes fragility curve.

The released hydrogen can ignite and lead to either a jet fire (in case of immediate ignition) or an explosion (in case of delayed ignition) (Groth and Hecht 2017a). In this work, jet fire is neglected because, given the layout considered, it cannot damage the reactor and its surrounding infrastructures, thanks to the presence of the fire walls surrounding each electrolyzer unit (Marchetti, Di Maio, Wismer, et al. 2025). With regards to explosion, we conservatively assume an undetected leakage to occur within the hydrogen piping system, so that the generated overpressure wave, modelled as in (Glover, Baird and Brooks 2020), can impact the above ground surrounding infrastructures, whose structural effects are modelled with the fragility curves in **Fig. 5** (for the switchyard and transmission tower) and **Fig. 6** (for the turbine building) in line with (Vedros et al. 2023).

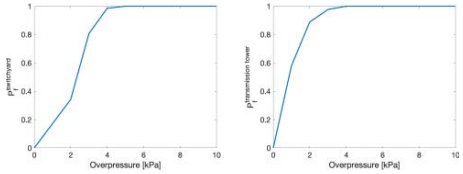

Fig. 5. Fragility curve of the switchyard (left) and transmission tower (right).

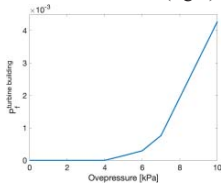

Fig. 6. Fragility curve of the turbine building.

The failure of the switchyard or the transmission tower leads to a Loss Of Offsite Power (LOOP), whereas the collapse of the turbine building leads to a Loss of Heat Sink (LHS).

- Steam leakage in the HES, which can be caused by the rupture of one of the steam pipes, the failure of one of the two reboilers or the rupture of one of the flow control valves. The fragility curves of the steam pipes are shown in **Fig. 7** and taken from (Jeon et al. 2022), whereas those of the reboilers and valves are shown in **Fig. 8**, respectively, taken from (Smith et al. 2006).

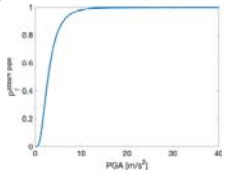

Fig. 7. Fragility curve of the steam pipes.

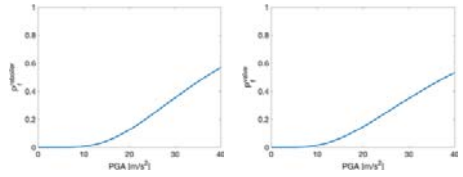

Fig. 8. Fragility curve of the reboiler (left) and flow control valve (right).

- Overcurrent event, which can be caused by the failure of the transformer, whose fragility

curve is shown in **Fig. 9** taken from (Vedros et al. 2023).

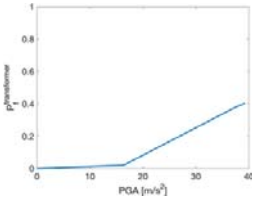

Fig. 9. Fragility curve of the transformer.

To protect the NPP turbine in case of overcurrent, three identical breakers are installed: one within the HTEF, one within the NPP protected area and one near the turbine. Each breaker consists of a parallel configuration of two relays in series with one high-voltage circuit breaker. In case of an unmitigated overcurrent event (i.e., failure of all breakers), the NPP turbine is damaged, leading to a LHS accident in which the heat extracted from the coolant is progressively reduced. The fragility curves of the relays and circuit breakers are shown in **Fig. 10**.

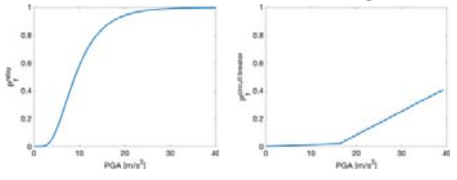

Fig. 10. Fragility curve of relay (left) and circuit breaker (right).

For the NPP, the earthquake can lead to:

- Loss Of Coolant Accident (LOCA), in case of failure of the coolant pipes, whose fragility is assessed using the fragility curve in **Fig. 11**, based on the fragility model presented in (Jeon et al. 2022).

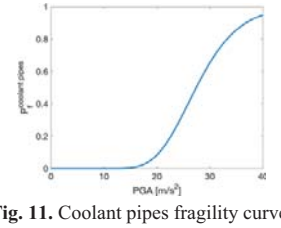

Fig. 11. Coolant pipes fragility curve.

- Main Steam Line Break (MSLB), in case of failure of the steam pipes, whose fragility is assessed using the fragility curve in **Fig. 7**.

To mitigate the escalation of the accidental scenarios and ensure a proper cooling of the reactor core, the NPP is equipped with four Emergency Core Cooling Systems (ECCSs) (one for each reactor unit) and two Emergency Diesel Generators (EDGs), to be used in case of LOOP. The failure probabilities P_f^{ECCS} and P_f^{EDG} are assessed using the fragility curves of **Fig. 12**, based on the fragility model presented in (Jeon et al. 2022).

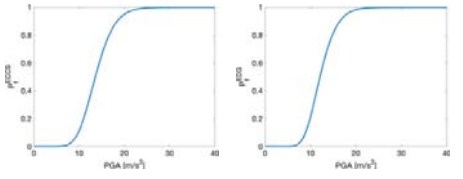

Fig. 12. Fragility curve of ECCS (left) and EDG (right).

The NPP is also equipped with a melting fuel plug (assumed to be always available) to drain the fuel in case of accidents. The time allowed to confirm that the drainage of the fuel from the reactor core through the melting fuel plug is successful is $T_s = 1200\ s$, that is therefore considered as the duration of the accidental scenario (Huke et al. 2015; Ilham and Okawa 2023). Inter-unit dependencies are considered and characterized by the Common Cause Failure (CCF) models presented in (Marchetti, Di Maio, and Zio 2025).

To assess the impact of the hazard on the system, the one-dimensional lumped parameter model presented in (Marchetti, Di Maio, and Zio 2025) is used to simulate safe and accidental conditions transients that might occur in the system following the occurrence of the IEs triggered by the earthquake hazard occurrence. The model consists of coupled neutronic and thermal-hydraulic models. The neutronic behaviour is described using a modified point-kinetics model with six delayed neutron groups, which accounts for fuel flow. The thermal-hydraulic model represents the heat transfer within the reactor core assuming that the fuel, piping wall, and coolant are each divided into three sections with lumped properties. The model

takes the failure times of the components and the safety systems as input and provides the peak cladding temperature $T_{w,i}$ of each $i = 1,2,3,4$ reactor unit as output, which are the safety parameters of interest here considered. The safety threshold not to be exceeded by $T_{w,i}$ during the accident is $T_{w,fail} = 1244\ K$ (Marchetti, Di Maio and Zio 2025).

3.3. Core damage frequency estimation

To estimate the core damage frequency, that measures the events per reactor-year of reactor core being damaged resulting in potential radioactive release, a MCS-IS procedure with M trials is enforced. The high-impact accidental scenarios of rare occurrence may otherwise not be sampled by standard MCS. IS is adopted to sample the PGA realizations from a biased importance distribution obtained via exponential tilting of the original hazard distribution in **Fig. 3**, which forces the HTEF-coupled NPP to be exposed to harsher ground acceleration conditions than expected. Specifically, the hazard curve is discretized into $K = 1000$ PGA levels x_k, each with associated natural probability, p_k, at the site of interest. The tilted importance distribution is defined as in (Asmussen and Glynn 2007):

$$q_k = \frac{p_k \exp(\beta \phi_k)}{C} \quad (1)$$

where $\beta = 20$ is a parameter that controls the strength of the bias, $C = \sum_{o=1}^{K} p_o \exp(\beta \phi_o)$ is a normalization term, and ϕ_k is a monotonically increasing function of the PGA, defined as:

$$\phi_k = \frac{x_k - x_{mean}}{x_{max} - x_{min}} \quad (2)$$

where x_{mean}, x_{max} and x_{min} are the mean, maximum and minimum values of the PGA natural distribution, respectively. For each *m-th* trial, $x_{k(m)}$ is sampled from the importance distribution, and the failure occurrences of the components and safety systems are sampled using the corresponding fragility curves. In case of hydrogen leakage, to assess whether hydrogen explosion occurs or not:

- the energy demand is sampled from the corresponding distribution (**Fig. 2**), to determine the HTEF operating conditions and the leak flow rate $\dot{m}_{leak,m}$ as in (Marchetti, Di Maio, Wismer, et al. 2025);
- the explosion occurrence is sampled using the Event Sequence Diagram (ESD) in (Groth and Hecht 2017b);
- the accumulation time $t_{acc,m}$ is sampled from a uniform distribution $t_{acc} \sim U(5,120)\ min$ (Glover et al. 2020), to determine the quantity of accumulated hydrogen and the corresponding explosion overpressure wave ρ_m;
- the failure of switchyard, transmission tower and turbine building are sampled from the corresponding fragility curves, when exposed to ρ_m.

The failure times of all components and safety systems are sampled from a uniform distribution along the whole accidental scenario duration. All information is, then, fed to the simulation model, which provides an output of $T_{w,i}^{m}$ for each simulation trial $m = 1,2, \dots, M$.

The core damage frequency is eventually calculated as follows:

$$F_{CDF} = \frac{1}{M} \sum_{m=1}^{M} \left[w_m \frac{1}{N} \sum_{i=1}^{N} 1\{T_{w,i}^{m} \geq T_{w,fail}\} \right] \quad (3)$$

where $1\{T_{w,i}^{m} \geq T_{w,fail}\}$ is a function equal to 1 when the failure criterion is met for the *i-th* reactor unit and 0 otherwise; w_m is the IS weight used to reweight samples drawn from the importance hazard distribution to ensure unbiased estimation under the original hazard distribution, and is defined as:

$$w_m = \frac{p_{k(m)}}{q_{k(m)}} \quad (4)$$

4. Results

Results obtained with $M = 10^6$ trials of MCS-IS are shown in **Fig. 13** and compared with those obtained with a standard MCS with 10^6 and

10^7 trials, where the latter is assumed as ground truth estimate. In addition to the estimated core damage frequency, **Fig. 13** reports the associated 95% Confidence Interval (CI).

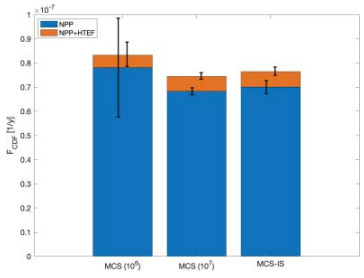

Fig. 13. Results (crude MCS vs MCS-IS).

It can be seen that the MCS-IS results are more conservative that the ground truth, whereas standard MCS with 10^6 trials is affected by larger uncertainty, which may lead to underestimation of the site-level risk increase. In particular, the integration of HTEF and NPP (combined orange and blue bars) yields an increase in core damage frequency (orange bar) of 9.24% with MCS-IS, compared with 6.63% using standard MCS with 10^6 trials and 9.09% by standard MCS with 10^7 trials, with respect to the baseline NPP-only risk estimates (blue bar). The standard MCS could, thus, underestimate the risk increase at the site level if an insufficient number of simulation trails were run. Also, as shown in **Fig. 13**, the variance (and the corresponding 95% CI) of the F_{CDF} estimated with the MCS-IS is significantly smaller than that obtained by standard MCS with 10^6 trials and comparable to that obtained by standard MCS with 10^7 trials. The corresponding percentage increase in core damage frequency ranges are $[7.3, 11.4]$ % for MCS-IS, $[0.9, 10.8]$ % for standard MCS (10^6 trials) and $[7.4, 11.0]$ % for standard MCS (10^7 trials). For a more comprehensive comparison, MCS-IS and standard MCS are evaluated in terms of three quantities: the sample standard deviation σ of F_{CDF}, the coefficient of variation $\delta = \sigma/F_{CDF}$ and the Figure Of Merit (FOM) of the method $FOM = 1/(\sigma^2 \cdot t_{comp})$, where t_{comp} is the computational time required by the method (Zio and Pedroni 2009). Results are reported in **Tab. 3**, which confirm the improved efficiency of MCS-IS in terms of variance reduction per unit computational time compared with standard MCS, as reflected by the larger FOM values.

Table 3. MCS-IS and standard MCS comparison.

Method	Trials	σ	δ	FOM
MCS	10^6	$1.3 \cdot 10^{-8}$	1.37	$8.2 \cdot 10^{11}$
	10^7	$1.4 \cdot 10^{-9}$	0.21	$7.1 \cdot 10^{12}$
MCS-IS	10^6	$2.2 \cdot 10^{-9}$	0.33	$2.8 \cdot 10^{13}$

From a licensing perspective, the results indicate that the integration of the HTEF leads to an increase in the estimated core damage frequency that would exceed acceptable licensing thresholds for the plant (U.S. Nuclear Regulatory Commission 2018). Therefore, to quantify the major contributor to the risk increase at the site level and inform, on this basis, appropriate design solutions, we quantify, only with respect to the MCS-IS results, the probability that each one of the HTEF IE occurrences (overcurrent, hydrogen leakage and steam leakage) leads to NPP core damage. This information can be extracted from the already simulated M scenarios by estimating the joint probability $P(IE \cap core\ damage)$ from the joint occurrence of the IE and core damage across MCS-IS trials, enabling a ranking of the dominant risk drivers. Then, as shown in **Fig. 14**, the main contributor is found to be the overcurrent. As an effective countermeasure, it might be suggested an increased redundancy and robustness of protection systems and circuit breaker logic, being these critical to mitigate the risk increase in such overcurrent scenarios.

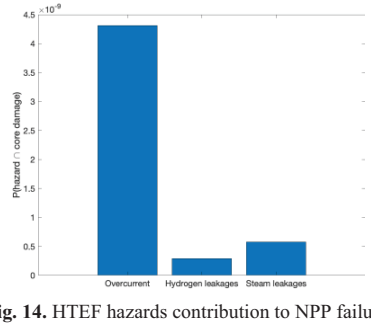

Fig. 14. HTEF hazards contribution to NPP failure.

5. Conclusions

In this work, we presented a computational risk assessment of an integrated energy system composed of a HTEF with an NPP coupled exposed to seismic hazard. The analysis allowed evaluating the risk increase on the nuclear side due to the coupling and identifying the dominant contributor among the HTEF IEs. A MCS-IS framework was implemented to efficiently generate the rare-event accident occurrences. The outcomes of the analysis highlight that overcurrent events are the dominant contributors to the estimated risk increase in the evaluated configuration, and therefore should be of primary consideration during early stage design.

References

Al-Douri, Ahmad, and Katrina M. Groth. 2024. "Hydrogen Production via Electrolysis: State-of-the-Art and Research Needs in Risk and Reliability Analysis." *International Journal of Hydrogen Energy* 63. https://doi.org/10.1016/j.ijhydene.2024.03.188.

Asmussen, S., and P. W. Glynn. 2007. *Stochastic Simulation: Algorithms and Analysis*. In *Analysis*, vol. 57.

Chalkiadakis, Nikolaos, Emmanuel Stamatakis, Melina Varvayanni, Athanasios Stubos, Georgios Tzamalis, and Theocharis Tsoutsos. 2023. "A New Path towards Sustainable Energy Transition: Techno-Economic Feasibility of a Complete Hybrid Small Modular Reactor/Hydrogen (SMR/H2) Energy System." *Energies* 16 (17). https://doi.org/10.3390/en16176257.

Energy Information Administration. 2023. *US Hourly Nuclear Energy Production Normalized Data. Available at: Https://Www.Eia.Gov/Electricity/Gridmonitor/Dashboard/Electric_overview/US48 US48/US 48*.

Frick, Konor, Daniel Wendt, Paul Talbot, Cristian Rabiti, and Richard Boardman. 2022. "Technoeconomic Assessment of Hydrogen Cogeneration via High Temperature Steam Electrolysis with a Light-Water Reactor." *Applied Energy* 306 (January): 118044. https://doi.org/10.1016/J.APENERGY.2021.118044.

Futalef, Juan Pablo, Francesco Di Maio, and Enrico Zio. 2025. "A Dynamic Importance Function for Accidental Scenarios Generation by RESTART in the Computational Risk Assessment of Cyber-Physical Infrastructures." *Reliability Engineering and System Safety* 253. https://doi.org/10.1016/j.ress.2024.110538.

Glover, Austin Micheal, Austin Ronald Baird, and Dusty Marie Brooks. 2020. *Hydrogen Plant Hazards and Risk Analysis Supporting Hydrogen Plant Siting near Nuclear Power Plants. SAN D2020-7946*.

Groth, Katrina M., Al-Douri Ahmad, Samantha Wismer, et al. 2024. *Quantitative Risk Assessment for Hydrogen Energy Systems: Part I Electrolyzers*.

Groth, Katrina M., and Ethan S. Hecht. 2017a. "HyRAM: A Methodology and Toolkit for Quantitative Risk Assessment of Hydrogen Systems." *International Journal of Hydrogen Energy* 42 (11). https://doi.org/10.1016/j.ijhydene.2016.07.002.

Groth, Katrina M., and Ethan S. Hecht. 2017b. "HyRAM: A Methodology and Toolkit for Quantitative Risk Assessment of Hydrogen Systems." *International Journal of Hydrogen Energy* 42 (11). https://doi.org/10.1016/j.ijhydene.2016.07.002.

Huke, Armin, Götz Ruprecht, Daniel Weißbach, Stephan Gottlieb, Ahmed Hussein, and Konrad Czerski. 2015. "The Dual Fluid Reactor - A Novel Concept for a Fast Nuclear Reactor of High Efficiency." *Annals of Nuclear Energy* 80. https://doi.org/10.1016/j.anucene.2015.02.016.

Ilham, Muhammad, and Tomio Okawa. 2023. "A Simple Analytical Model to Predict the Freeze Plug Opening Time in Molten Salt Reactors." *Journal of Nuclear Engineering and Radiation Science* 9 (4). https://doi.org/10.1115/1.4062879.

International Energy Agency. 2022. *Global Hydrogen Review*.

Jeon, Bub Gyu, Sung Wan Kim, Da Woon Yun, Daegi Hahm, and Seunghyun Eem. 2022. "Seismic Fragility Evaluation of Main Steam Piping of Isolated APR1400 NPP Considering the Actual Failure Mode." *Sustainability (Switzerland)* 14 (14). https://doi.org/10.3390/su14148315.

Liu, Chunyu, Run Luo, and Rafael Macián-Juan. 2021. "A New Uncertainty-Based Control Scheme of the Small Modular Dual Fluid Reactor and Its Optimization." *Energies* 14 (20). https://doi.org/10.3390/en14206708.

Marchetti, Stefano, Francesco Di Maio, Samantha E. Wismer, Katrina M. Groth, and Enrico Zio. 2025. "Preliminary Hazard Analysis for Hydrogen Production by Coupled High Temperature Electrolysis Facilities and Nuclear Power Plants." *Proceedings of the 35th European Conference on Safety and Reliability (ESREL 2025)*.

Marchetti, Stefano, Francesco Di Maio, and Enrico Zio. 2025. "An Integrated Deterministic and Probabilistic Safety Assessment of Multi-Unit Small Modular Reactors Considering the Degradation of Shared Safety Barriers." *Nuclear Science and Engineering*, ahead of print. https://doi.org/https://doi.org/10.1080/00295639.2025.2515349.

Moura, João, and Isabel Soares. 2023. "Financing Low-Carbon Hydrogen: The Role of Public Policies and Strategies in the EU, UK and USA." *Green Finance* 5 (2). https://doi.org/10.3934/GF.2023011.

Pedroni, Nicola, and Enrico Zio. 2017. "An Adaptive Metamodel-Based Subset Importance Sampling Approach for the Assessment of the Functional Failure Probability of a Thermal-Hydraulic Passive System." *Applied Mathematical Modelling* 48. https://doi.org/10.1016/j.apm.2017.04.003.

Rubinstein, Reuven Y. 1997. "Optimization of Computer Simulation Models with Rare Events." *European Journal of Operational Research* 99 (1). https://doi.org/10.1016/S0377-2217(96)00385-2.

Shahraki, H., and N. Shabakhty. 2015. "Seismic Performance Reliability of RC Structures: Application of Response Surface Method and Systemic Approach." *Civil Engineering Infrastructures Journal* 48 (1).

Smith, Curtis, Scott Beck, and William Galyean. 2006. "Separation Requirements for a Hydrogen Production Plant and High-Temperature Nuclear Reactor." *Proceedings of the 2006 International Congress on Advances in Nuclear Power Plants, ICAPP'06* 2006.

Turati, Pietro, Nicola Pedroni, and Enrico Zio. 2016. "Advanced RESTART Method for the Estimation of the Probability of Failure of Highly Reliable Hybrid Dynamic Systems." *Reliability Engineering and System Safety* 154. https://doi.org/10.1016/j.ress.2016.04.020.

U.S. Department of Energy. 2023. *U.S. National Clean Hydrogen Strategy and Roadmap*. https://www.hydrogen.energy.gov/library/roadmaps-vision/clean-hydrogen-strategy-roadmap.

U.S. Nuclear Regulatory Commission. 2018. *An Approach for Using Probabilistic Risk Assessment in Risk-Informed Decisions on Plant-Specific Changes to the Licensing Basis*. no. Regulatory Guide 1.174, Revision 3.

Vedros, Kurt G., Robby Christian, and Courtney Otani. 2023. *Expansion of Hazards and Probabilistic Risk Assessments of a Light-Water Reactor Coupled with Electrolysis Hydrogen Production Plants. INL/RPT-23-74319-Rev000*.

Westover, Tyler, and Richard Boardman. 2023. *Preconceptual Designs of Coupled Power Delivery between a 4-Loop PWR and 100-500 MWe HTSE Plants. INL/RPT-23-71939-Rev001*.

Yanxing, Zhao, Gong Maoqiong, Zhou Yuan, Dong Xueqiang, and Shen Jun. 2019. "Thermodynamics Analysis of Hydrogen Storage Based on Compressed Gaseous Hydrogen, Liquid Hydrogen and Cryo-Compressed Hydrogen." *International Journal of Hydrogen Energy* 44 (31). https://doi.org/10.1016/j.ijhydene.2019.04.207.

Zio, E, and N. Pedroni. 2009. "Subset Simulation and Line Sampling for Advanced Monte Carlo Reliability Analysis." In *Reliability, Risk, and Safety*. https://doi.org/10.1201/9780203859759.ch94.

Zio, Enrico. 2013. *The Monte Carlo Simulation Method for System Reliability and Risk Analysis*. Springer.